Available online at www.sciencedirect.com
SCIENCE DIRECT®

Journal of the European Ceramic Society 23 (2003) 1957–1962
www.elsevier.com/locate/jeurceramsoc

Corrosion behavior and strength degradation of Ti_3SiC_2 exposed to a eutectic K_2CO_3 and Li_2CO_3 mixture

Guangming Liu*, Meishuan Li, Yanchun Zhou, Yaming Zhang

Shenyang National Laboratory for Materials Science, Institute of Metal Research, Chinese Academy of Sciences, Shenyang 110016, China

Received 28 June 2002; received in revised form 10 October 2002; accepted 20 October 2002

Abstract

The corrosion of polycrystalline Ti_3SiC_2 was studied in the eutectic Li_2CO_3 (68 at.%) and K_2CO_3 (32 at.%) mixture at 650–850 °C. Ti_3SiC_2 exhibited better corrosion resistance at 650 °C. However, the mass loss was fast when temperature was above 700 °C. It was demonstrated that the surface chemical reaction-controlled shrinking core model could be applied to describe the relationship between the degree of the corrosion and reaction time for the corrosion of Ti_3SiC_2 in the 700–850 °C temperature range. The corresponding apparent activation energy was 206 kJ/mol. Corrosion resulted in roughness of specimen surface. The fracture strength of the corroded samples was evaluated by a three-point bending test. The results showed that the degradation of the fracture strength was about 25% of the original values for the corroded specimens up to 10% weight loss. The mechanism of the strength degradation was discussed based on the analysis of the microstructure and composition of the corroded sample.
© 2003 Elsevier Science Ltd. All rights reserved.

Keywords: Carbonate melt; Corrosion; Fracture strength; Molten salts; Ti_3SiC_2

1. Introduction

Ti_3SiC_2 with a layered crystal structure possesses a combination of the properties of both metals and ceramics. The unique properties of Ti_3SiC_2 include high strength and modulus, damage tolerance at room temperature, excellent thermal shock resistance, good electrical and thermal conductivities, easy machinability, good oxidation resistance, and low density. These unusual combination of the properties render it a candidate structural material for high temperature applications.[1–6] When oxidized in air, a protective oxide scale formed in layers, where the inner layer was composed of a mixture of SiO_2 and TiO_2 and the outer layer was pure TiO_2. It showed a parabolic oxidation kinetics in air in the 900–1300 °C temperature range with an activation energy of about 370 kJ/mol.[7]

Use of this material at high temperatures commonly entailed exposure to molten salts, especially, sodium sulphate (Na_2SO_4) and sodium carbonate (Na_2CO_3). It is necessary to investigate the hot corrosion behavior of this material. We studied the hot corrosion behavior of Ti_3SiC_2 induced by Na_2SO_4.[8] However, up to now, investigation focused on the hot corrosion resistance of this material was seldom reported. The separator plates in molten carbonate fuel cell (MCFC) are subjected to corrosive carbonate environment. It is reported that non-oxide ceramic, for example, TiN, TiC and Ce-based ceramics, might be suitable coating material of separator because of their low ionic and high electronic conductivity compared with oxide materials.[9] Compared to the earlier mentioned ceramics, Ti_3SiC_2 combined a high oxidation resistance and better electronic conductivity, which was considered as a potential material for separator plates. However, no data on the hot corrosion of Ti_3SiC_2 in Li_2CO_3–K_2CO_3 are now available. In the present paper, the hot corrosion behavior of Ti_3SiC_2 in the Li_2CO_3–K_2CO_3 eutectic mixture in air at 650–850 °C was reported. On the other hand, the hot corrosion attack might greatly affect the mechanical properties of the high temperature structural ceramic. However,

* Corresponding author. Tel.: +86-24-23915913; fax: +86-24-23891320.
E-mail address: gmliu@imr.ac.cn (G. Liu).

0955-2219/03/$ - see front matter © 2003 Elsevier Science Ltd. All rights reserved.
PII: S0955-2219(02)00419-3

the effect of corrosion on the mechanical properties of Ti_3SiC_2 has not been fully investigated because most of studies have been focused on the synthesis process and oxidation behavior of this material. From the point of view of strength degradation to evaluate corrosion resistance is important for applying this material to structural application in corrosive environments. The results are useful for selecting the appropriate conditions for the application of this technologically important material.

2. Experimental

2.1. Specimen preparation

Ti_3SiC_2 used in this work was TSC^{ZS510}, which was fabricated by the in-situ hot pressing/solid-liquid reaction process.[10] Briefly, Ti, Si, and graphite powders were mixed and milled in a polypropylene jar for 10 h. After ball milling, the mixture was cold pressed in a graphite die with the diameter of 50 mm. The in-situ hot pressing/solid–liquid reaction was performed under a flowing argon atmosphere in a furnace using graphite as heating element. The furnace temperature was rapidly increased to 1550° at the rate of 40°/min, then the sample was held at the temperature for 1 h under a pressure of 40 MPa and then cooled down with the pressure removed.

Rectangular specimens with dimensions of 3×4×36 mm bars were cut by the electrical-discharge method. The surfaces were polished down to 800 alumina paper. The specimens were cleaned in acetone, ethanol, and distilled water in an ultrasonic bath before tests.

2.2. Specimen examination

The mixed carbonate powders were prepared according to the Li_2CO_3:K_2CO_3 molar ratios of 0.68:0.32. The samples and mixed carbonate powders were put into an Al_2O_3 crucible, and then it was placed in a box furnace in air. The tests were conducted in the 650–850 °C temperature range.

After hot corrosion tests, the samples were washed with boiled distilled water to dissolve the remains of carbonate and other dissolvable salts. The fracture strength of the corroded specimens was determined at room temperature by three point bending tests with a span length of 30 mm and cross-head speed of 0.5 mm/min.

The microstructure analysis on outer surfaces and polished cross section of corroded specimens were carried out by using a scanning electron microscope (SEM) equipped with an energy dispersive spectroscope (EDS). The phase compositions of the corroded layer were determined by X-ray diffraction (XRD).

3. Results and discussion

3.1. Kinetics of hot corrosion in the eutectic K_2CO_3–Li_2CO_3 mixture

Fig. 1 shows the fraction of weight loss (α) as a function of time for hot corrosion of Ti_3SiC_2 in the eutectic K_2CO_3–Li_2CO_3 mixture in the 650–850 °C temperature range. The weight loss of specimens extremely increased with increasing temperature. A significant weight loss of Ti_3SiC_2 was observed at 800 and 850 °C. In contrast the weight loss was considerably low at 650 °C. Because the volume of sample would shrink continuously during the corrosion, the hot corrosion behavior of this material could be described by the shrinking core model. In the heterogeneous reaction systems such as solid and liquid phases, if the surface chemical process was rate limiting, according to the shrinking core model the relationship between the fractional conversion (α) and time was expressed by the following equation.[11]

$$1-(1-\alpha)^{1/3}=kt/r_0 \quad (1)$$

where α is fractional conversion, t is time, r_0 is the radius of the sample, k is the rate constant. As the specimens used in the present work were rectangular coupons, r_0 is defined as $3abc$ / 2 $(ab+bc+ac)$, where a is the specimen width, b is specimen thickness, c is the specimen length, respectively.

As illustrated in Fig. 2, the corrosion time had a linear relationship with $1-(1-\alpha)^{1/3}$ in the test temperature range, consequently, the relation between time and fractional conversion of Ti_3SiC_2 in $(Li_{0.68}K_{0.32})_2CO_3$ melts followed the surface chemical reaction-controlled shrinking core model.

Fig. 3 is the Arrhenius relation between the rate constants and temperature of Ti_3SiC_2 corroded in the eutectic K_2CO_3–Li_2CO_3 mixture. The corresponding apparent activation energy was determined to be 206

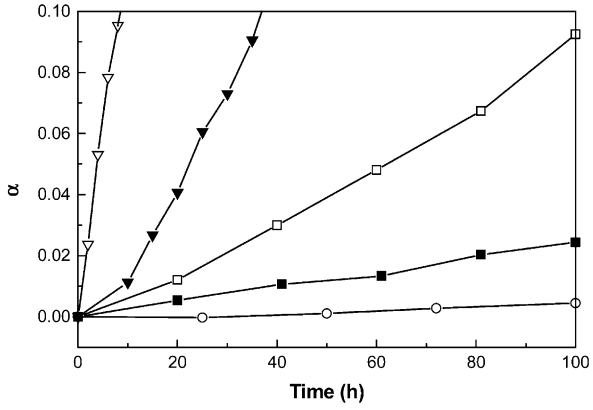

Fig. 1. The fraction of weight loss (α) as a function of time for hot corrosion of Ti_3SiC_2 in the mixed carbonate melts at various temperatures. (○) 650 °C, (■) 700 °C, (□) 750 °C, (▼) 800 °C, (▽) 850 °C.

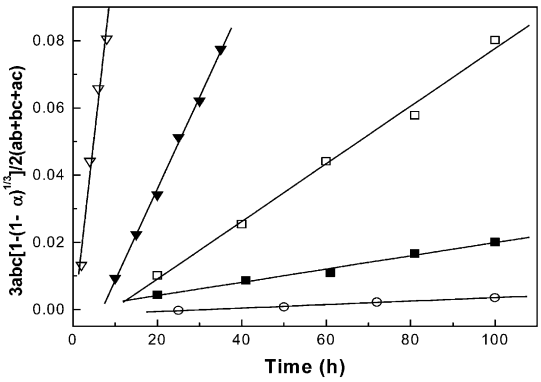

Fig. 2. Plots of $3abc[1-(1-\alpha)^{1/3}]/2(ab+bc+ac)$ versus time for Ti_3SiC_2 corroded in $(Li_{0.68}K_{0.32})_2CO_3$ melts at various temperatures. (○) 650 °C,(■) 700 °C, (□) 750 °C, (▼) 800 °C, (▽) 850 °C.

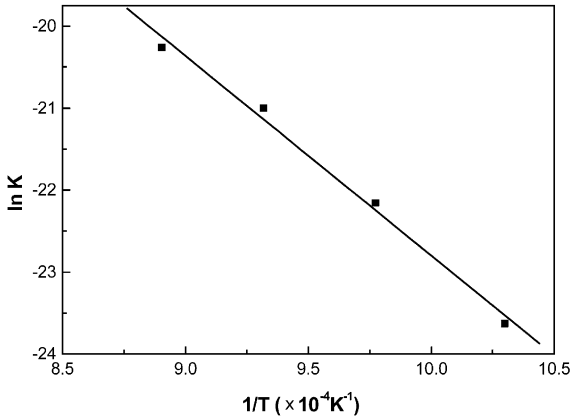

Fig. 3. Arrhenius relationship between the rate constants and temperature for Ti_3SiC_2 corroded in $(Li_{0.68}K_{0.32})_2CO_3$ melts.

kJ/mol. This value was lower than that of 350 kJ/mol for oxidation of Ti_3SiC_2 in air.[7] Therefore, Ti_3SiC_2 was susceptible to hot corrosion attack by $(Li_{0.68}K_{0.32})_2CO_3$ melts, especially, the dramatic corrosion was observed when the temperature was above 800 °C, although it exhibited good oxidation resistance up to 1100 °C in air.

3.2. Phase composition and microstructure of the corrosion products

Fig. 4(a) and (b) shows the surface microstructure of Ti_3SiC_2 after hot corrosion in mixed carbonate melt for 100 h at 650 °C and 40 h at 800 °C, respectively. The samples corroded at 700, 750, and 850 °C had the similar surface microstructure to 800 °C (not shown here). Some pores were observed in the microstructure of the corroded sample surface. With temperature increasing, the pores existed in Fig. 4(b) were bigger than that in Fig. 4(a).

Fig. 5(a), (b), (c) and (d) are cross section microstructure of specimens corroded at 650, 700, 800 and 850 °C, respectively. SEM observation revealed that all of the cross sections had pits. It is noteworthy that most of the pits in the surface were shallow. The mechanism of

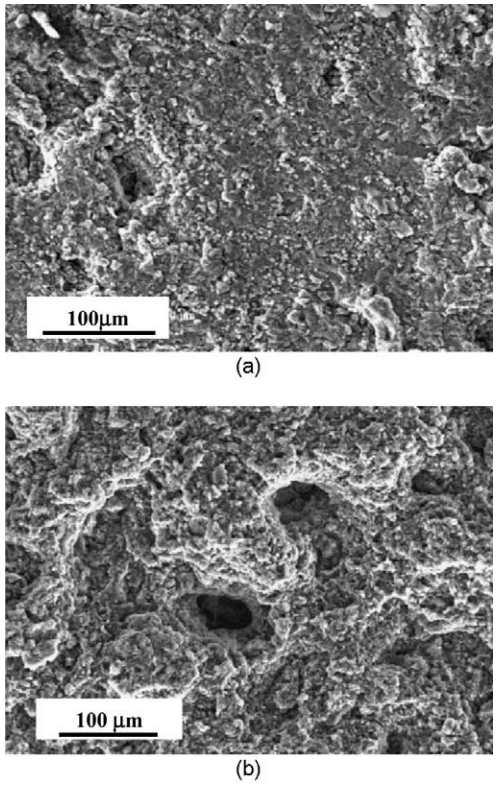

Fig. 4. The surface morphology of Ti_3SiC_2 after hot corrosion in a mixture of K_2CO_3 and Li_2CO_3 melts (a) at 650 °C for 100 h; (b) at 800 °C for 40 h.

formation of this type of shallow pits in substrate might be related to the microstructure characteristics of Ti_3SiC_2. Ti_3SiC_2 was a ternary layered compound. Similar to most other ceramics, a number of pores and large grain boundaries existed in the bulk materials (the porosity of Ti_3SiC_2 used in the tests is about 2 vol.%). Those pores and large boundaries could serve as the short paths for inward diffusion of carbonate melts. In these areas corrosion rate was fast and led to pits formation.

Fig. 6 shows the X-ray diffraction patterns of corroded sample at 650 and 850 °C, respectively. Combining the results of XRD and EDS analysis, we reasonably concluded that the main corroded phases of corroded layer were identified as $TiO_{1.04}$ and Li_2TiO_3. However, EDS analysis revealed that the elements in corroded layer were Ti, O, Si, Li. The reason for the fact that no crystalline Si-containing phase was detected was assumed due to that the content of SiO_2 in the corrosion film was too low or SiO_2 was not in crystalline form. Similar phenomenon was observed in Ti_3SiC_2 oxidized at 1100–1300°, where Si was detected by EDS but no reflections of SiO_2 were identified by XRD.[7]

3.3. Hot corrosion mechanism of Ti_3SiC_2

The mechanisms of hot corrosion have been studied in detail for SiC and Si_3N_4, however, less information is

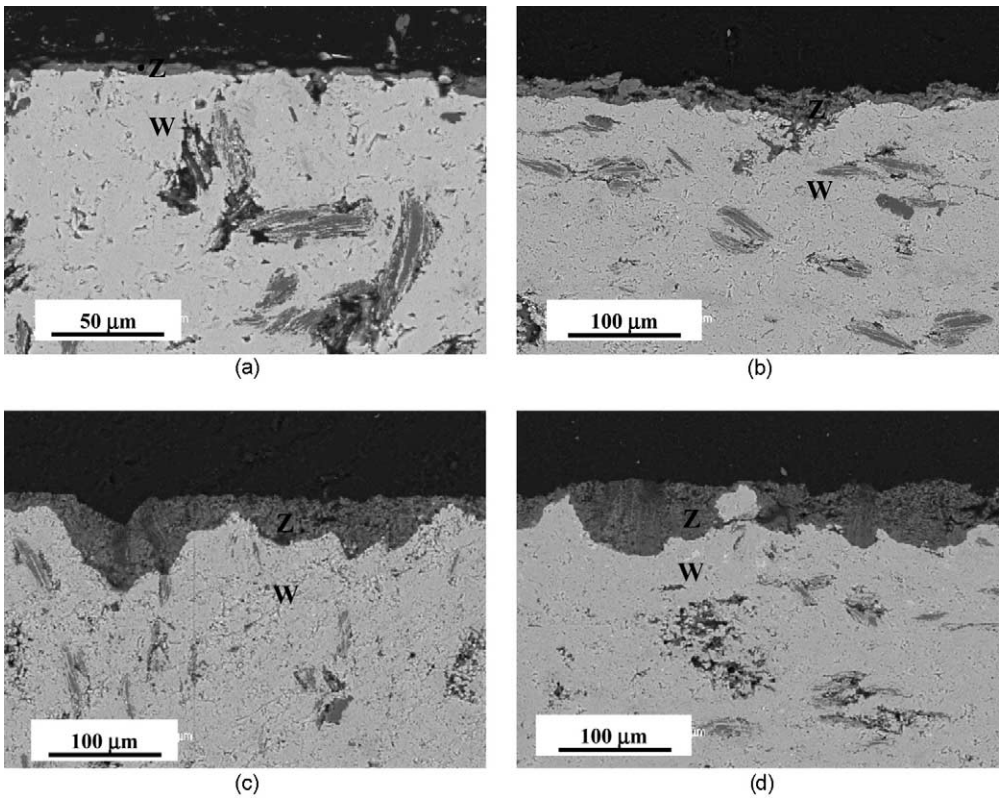

Fig. 5. The cross sections of Ti_3SiC_2 corroded in molten carbonate at various temperatures (a) at 650 °C for 100 h; (b) at 700 °C for 100 h; (c) at 800 °C for 40 h; (d) at 850 °C for 8 h (Z is corroded layer; W is substrate).

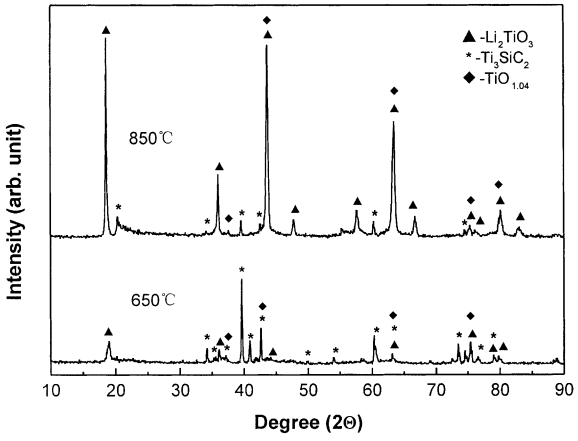

Fig. 6. XRD pattern of samples corroded in $(Li_{0.68}K_{0.32})_2CO_3$ melts (a) at 650 °C for 100 h; (b) at 850 °C for 8 h.

available for Ti_3SiC_2. It was reported that the presence of oxygen accelerated the reaction between non-oxide ceramics and carbonates, for example silicon carbide, silicon nitride, and aluminum nitride ceramics immersed in potassium sulfate–potassium carbonate melts in air at 1013–1200 °C, the corrosion rate increased obviously.[12] During the hot corrosion two main rate-determining process were considered in some detail:[13] (1) transport of oxidant from the gas phase through the molten salts and the corrosion products to the site of active oxidation, (2) dissolution/reprecipitation of oxide within the corrosion product layer owing to a solubility gradient. It was concluded that fluxing was very likely to be rate controlling in the early stages of hot corrosion, but later, when the actual hot corrosion rate had increased considerably, oxidant transport was controlling. The distribution of salt within the pores of the scale changes with time, and this was a key issue in determining the rate of reaction.

It was considered that silicon carbide did not react with Li_2CO_3 and K_2CO_3 directly.[14] Similarly, the weight loss of the Ti_3SiC_2 ceramic in the eutectic K_2CO_3–Li_2CO_3 mixture was caused by the dissolution of SiO_2 and TiO_2, which formed by the oxidation of Ti_3SiC_2 owing to dissolved oxygen.[7]

$$Ti_3SiC + 5O_2 = 3TiO_2 + SiO_2 + 2CO \quad (2)$$

On the other hand, Li_2CO_3 was much more basic than K_2CO_3, for example, the activities of Li_2O and K_2O in the eutectic mixture was 6.5×10^{-6} and 5.5×10^{-15} at 650 °C, respectively.[15] Therefore, mainly Li-containing corrosion products were formed according to the following reactions:[9]

$$Li_2CO_3(l) + SiO_2 = Li_2O\cdot SiO_2 + CO_2(g) \quad (3)$$

$$Li_2CO_3(l) + TiO_2 = Li_2O\cdot TiO_2 + CO_2(g) \quad (4)$$

The oxidation protection of Ti_3SiC_2 depended on oxide scale TiO_2 and SiO_2. It was shown that molten

salts dissolved this oxide layer according to the earlier reactions. Therefore, corrosion attack of Ti_3SiC_2 was accelerated in the eutectic K_2CO_3–Li_2CO_3 mixture.

As mentioned earlier, oxygen in molten salt was consumed continuously according to reaction 2. Oxygen transport became a controlling process. Under this condition, oxygen was insufficient to sustain the oxidation of Ti_3SiC_2 at the substrate/molten salt interface, where oxygen partial pressure was too low to form TiO_2. For this reason Ti_3SiC_2 was oxidized to form $TiO_{1.04}$, which was identified by XRD.

3.4. Degradation of fracture strength for corroded specimen

The bending strength of Ti_3SiC_2 after corrosion test in mixed $(Li_{0.68}K_{0.32})_2CO_3$ melts as a function of mass loss was shown in Fig. 7. As discussed earlier, the corrosion of Ti_3SiC_2 ceramics by mixed carbonate melts resulted in rough surface and pits of the specimens, which degraded the fracture strength. The fracture strength of the specimens corroded in the carbonate melts was determined by a three-point bending test according to the following equation.

$$\sigma_{3b} = 3PL/2ab^2 \quad (5)$$

where P is the load to failure, L is the span length, a is the specimen width and b is the thickness. The dimensions of a and b were measured on the unpolished corroded specimens.

A significant strength degradation was detected at the early stage of corrosion. The initial average strength reduction was estimated to be about 25%. The degradation of strength of the corroded specimen strongly depended on the pits of the sample surface.[16] The shallow pits indicated that pits did not deepen dramatically with increasing temperature although the corrosion rate increased rapidly. The whole corrosion was controlled by both pitting corrosion and general overall corrosion.

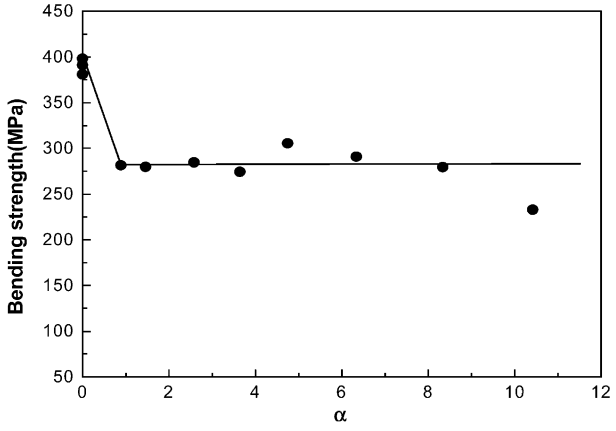

Fig. 7. Bending strength plotted against weight loss after corrosion test.

Therefore, after the initial stage no noticeable degradation of strength was observed up to 10% of mass loss. However, more detailed studies are obviously needed to determine the dominant mechanism. It is noteworthy that determining a relationship between strength and flaw size generated during corrosion tests is very important for understanding the failure mechanism.

4. Conclusions

1. Ti_3SiC_2 suffered serious hot corrosion attack in the mixed K_2CO_3–Li_2CO_3 eutectic mixture in the 700–850° temperature range. However, corrosion rate was visibly slow at 650 °C. The surface chemical reaction-controlled shrinking core model fully described the relationship between the degree of the corrosion and reaction time. The corresponding apparent activation energy was determined to be 206 kJ/mol.
2. The specimen suffered pitting attack during corrosion in the mixed K_2CO_3–Li_2CO_3 eutectic mixture. The main corrosion products, which adhered on the corroded specimen, were identified as $TiO_{1.04}$ and Li_2TiO_3.
3. The strength degradation was observed for Ti_3SiC_2 after corrosion in the eutectic K_2CO_3 and Li_2CO_3 mixture at the initial corrosion. The main reason was connected to both pitting attack and general overall corrosion of the substrate.

Acknowledgements

This work was sponsored by National Outstanding Young Scientist Foundation of China for Y. C. Zhou under Grant No.59925208 and State Key Laboratory for Corrosion and Protection of Metals.

References

1. Lis, J., Miyamoto, Y., Pampuch, R. and Tanihata, K., Ti_3SiC_2-based materials prepared by HIP-SHS techniques. *Mater. Lett.*, 1995, **22**, 163–168.
2. Sun, Z. M. and Zhou, Y. C., Synthesis of Ti_3SiC_2 powders by a solid-liquid method. *Scripta Mater.*, 1999, **41**(1), 61–66.
3. Tong, X., Yano, T. and Iseki, T., Synthesis and mechanical properties of Ti_3SiC_2/SiC composites. *J. Mater. Sci.*, 1995, **30**, 3087–3090.
4. Zhou, Y. C. and Sun, Z. M., Microstructure and mechanism of damage tolerance for Ti_3SiC_2 bulk ceramics. *Mater. Res. Innovat.*, 1999, **2**(6), 360–363.
5. Arunajatesan, S. and Carim, A. H., Synthesis of titanium silicon carbon. *J. Am. Ceram. Soc.*, 1995, **78**, 667–672.
6. Zhou, Y. C. and Sun, Z. M., Micro-scale deformation of polycrystalline Ti_3SiC_2 under room temperature compression. *J. Eur. Ceram. Soc.*, 2001, **21**(8), 1007–1010.

7. Sun, Z. M., Zhou, Y. C. and Li, M. S., Oxidation behavior of Ti_3SiC_2-based ceramic at 900–1300 °C in air. *Corr. Sci.*, 2001, **43**, 1095–1109.
8. Liu, G. M., Li, M. S., Zhou, Y. C. Hot corrosion of Ti_3SiC_2-based ceramics superficially coated with Na_2SO_4 at 900 °C and 1000 °C in air. *Corr. Sci.* in press.
9. Keijzer, M., Hemmes, K., Van Der Put, P. J. J. M., De Wit, J. W. and Schoonman, J., A search for suitable coating materials on separator plates for molten carbonate fuel cells. *Corr. Sci.*, 1997, **39**, 483–494.
10. Zhou, Y. C., Sun, Z. M., Chen, S. Q. and Zhang, Y., In-situ hot pressing/solid-liquid reaction synthesis of dense Ti_3SiC_2 bulk ceramics. *Mater. Res. Innovat.*, 1998, **2**(3), 142–146.
11. Sato, T., Koike, Y., Endo, T. and Shimada, M., Corrosion and strength degradation of Si_3N_4 and sialons in K_2CO_3 and K_2SO_4 melts. *J. Mater. Sci.*, 1998, **23**, 1405–1410.
12. Tsugio, S., Yoshimi, K. and Masahiko, S., Corrosion of SiC, Si_3N_4 and AlN in the molten K_2SO_4–K_2CO_3 salts. *International Journal of High Technology Ceramics*, 1986, **2**(4), 279–290.
13. Lee, K. N. and Shores, D. A., Transport considerations in the hot corrosion of Ni by molten alkali carbonates. *J. Electrochem. Soc.*, 1990, **137**, 859–871.
14. Sato, T., Kubota, K. and Shimada, M., Corrosion and strength degradation of sintered α-SiC in K_2CO_3 melts. *J. Mat. Sci. Lett.*, 1991, **10**, 789–791.
15. Spiegel, M., Biedenkopf, P. and Grabke, J. J., Corrosion of iron base alloys and high alloy steels in the Li_2CO_3–K_2CO_3 eutectic mixture. *Corr. Sci.*, 1997, **39**(7), 1193–1210.
16. Hancock, P., Chubb, J. P., Colenbie, B. and Finnigan, J. W., Hot corrosion of α silicon carbide and β silicon nitride. *Werkstoffe und Korrosion.*, 1990, **41**, 743–748.